Simulation of bulk piezoelectric implant with amplitude modulation-based backscatter communication for implant applications

Muhammad Junaid Akhtar
Electrical and Electronics Engineering
Koç University
Istanbul, Turkey
muhammadakhtar20@ku.edu.tr

Alp Timuçin Toymuş
Mechanical Engineering
Koç University
Istanbul, Turkey
atoymus21@ku.edu.tr

Levent Beker
Mechanical Engineering
Koç University
Istanbul, Turkey
lbeker@ku.edu.tr

2021 IEEE International Ultrasonics Symposium (IUS) | 978-1-6654-0355-9/21/$31.00 ©2021 IEEE | DOI: 10.1109/IUS52206.2021.9593728

***Abstract*—Recently, ultrasound has been used for power transfer and backward data transmission from implantable medical devices. Backward data communication is typically based on the amplitude modulation of the backscattered signal with changing electrical load of the implant. Contrary to its importance, the sensitivity of the backscattered voltage with reference to the electrical load has not been quantitatively determined yet. This work presents the results of transient simulations and shows the increasing trend in echo voltage with the increasing load resistance. Additionally, simulation studies indicate a decreasing sensitivity of echo voltage to load resistance with increasing backing impedance of the implant.**

Keywords—Implants, Acoustics, Backscatter, Circuit model, Echo modulation, Piezoelectric, Ultrasound

I. Introduction

Ultrasonic mm-scale implants have recently been proposed for a variety of implanted medical devices. These devices monitor physiological signals, such as pressure, temperature, blood oxygen saturation, and tissue impedance [1]. Implantable medical devices (IMDs) are being extensively employed to stimulate the nervous system and neural recordings [2]. The extraction of data and communication with the IMD is a key design aspect. Wires are cumbersome, aesthetically unpleasant, and might cause infection. They can also cause electromagnetic interference and crosstalk [3]. Therefore, wireless communication with an IMD has become essential.

Different protocols have been used for ultrasonic backward data transfer. One method of obtaining backward data from the implant was suggested by Ozeri et al. [4]–[6] in which a pair of coupled inductors were employed, in addition to the piezoelectric elements. This method wastes precious space in the IMD. In another method using a single transducer [7], the impedance of the implanted transducer was altered between open circuit and 50 Ω. A switched capacitor was used to modulate the electrical impedance of the implanted transducer in [8], which would cause a complete reflection from the transducer to mark a data bit of ‘‘1’’.

Backward data transfer is typically achieved through impedance modulation. A change in the electrical load of the IMD alters the acoustic reflection coefficient of an implanted bulk piezoelectric ceramic (PC), which leads to amplitude modulation of the backscattered signal. Therefore, understanding the relationship between the shunt impedance at the electrical port of the IMD and the amplitude modulation of the backscattered signal is a critical part of the design process. The objective of this research was to determine the sensitivity of the backscattered voltage to the variations of the electrical load quantitatively.

II. Methods

A. Piezoelectric Equivalent Circuit Model

For modeling a piezoelectric transducer, various equivalent circuit models have been presented over the years. Mason [9] presented an exact equivalent circuit that separated the piezoelectric material into an electrical port and two acoustic ports through an ideal electromechanical transformer [10]. The problem with the model is the presence of negative capacitance. Redwood model [11] removed this negative capacitance and transformed it to the acoustic side of the transformer. KLM [12] model removed circuit elements between the top of the transformer and the node of the transmission line.

A disadvantage of the transformer is that it does not allow flexibility, and it is frequency-dependent. Both the unphysical negative capacitance and use of transformer were avoided by the Leach model [13], which employs controlled sources instead of the transformer to model the coupling between the electrical and the mechanical systems. Here, we have used the Leach model because it is SPICE (Simulation Program with Integrated Circuit Emphasis) friendly. The Leach model for thickness mode transducer is shown in Fig. 1.

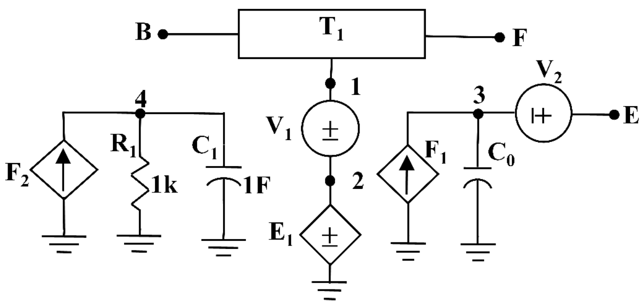

Fig. 1. Leach model for thickness mode transducer [13].

T_1 is a transmission line with an impedance equal to the characteristic impedance of the transducer and electrical delay equal to the time taken by sound waves to travel through the thickness of the transducer. Here C_0 is the capacitance of the transducer at resonance. The dependent source F_1 has value hC_0 where and F_1 has value h, where h is the piezoelectric constant. Values of R_1 and C_1 are fixed at R_1=1 kΩ and C_1=1 F. The node labels E, B, and F denote the electrical, back, and front ports, respectively.

B. *Ultrasonic Backscatter Communication Channel*

A typical ultrasonic backscatter communication channel is shown in Fig. 2(a). It consists of an external transducer, a matching layer, a propagation medium, and an implanted bulk piezoelectric ceramic (PC) [1]. For simplicity, we omit the external transducer and matching layer, which serve to deliver voltage excitation to and from the PC through the propagation medium, i.e., tissue.

In our simulations, we replace the external transducer and matching layer with an equivalent driving circuit connected to the front acoustic port of tissue, having acoustic impedance (Z_F). The equivalent circuit used in the simulation is shown in Fig. 2(b). The link operating frequency is chosen to be the resonant frequency of the implant piezo because the piezo has the highest electromechanical transduction efficiency and exhibits a resistive internal impedance at resonance [1].

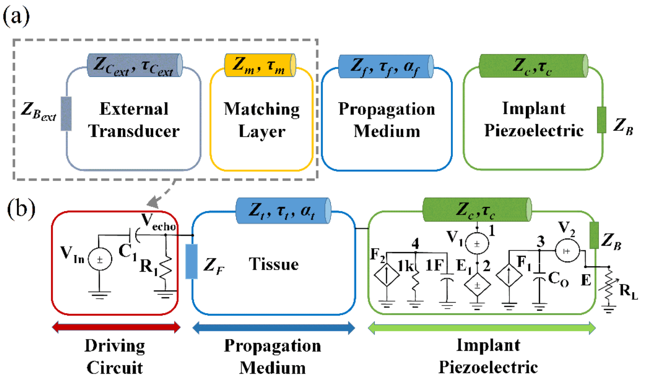

Fig 2. (a) Typical ultrasonic backscatter communication channel. (b) The equivalent circuit used in simulations.

The propagation of sound waves in the tissue layer is simulated by using a lossy transmission line model. The parameters of the lossy transmission line are as follows [14]:

$$R = 2\rho v A \alpha \quad (1)$$

$$L = A\rho \quad (2)$$

$$C = \frac{1}{A\rho v^2} \quad (3)$$

Where ρ is the density of tissue and v is the speed of sound in tissue. A is the cross-sectional area of the implanted piezoelectric and α is the co-efficient of attenuation inside the tissue.

III. Simulation

Transient simulations were carried out in LTSPICE to analyze the amplitude fluctuations of the backscattered signals by varying the resistive load at the electric port of the implanted PC. Piezoceramic cube (APC 851) has been used as the implant in the simulations. Air was used as a backing layer for the PC. The circuit is excited by 10 square pulses at the resonant frequency of the piezo cube. The implemented circuit schematic is shown in Fig. 3. Details of other parameters used in the simulation are shown in Table 1.

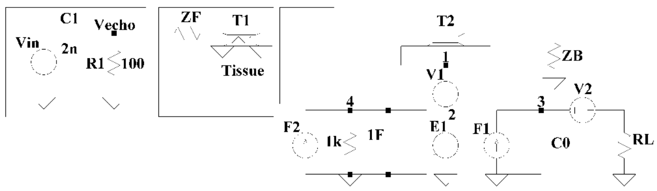

Fig. 3. Circuit Implementation in LTSPICE.

TABLE 1. Parameters used in the simulation.

Parameter	Description	Value	Units
ρ	Piezo density	7500	$Kg.m^{-3}$
s_{33}^{D}	Piezo open-circuit elastic compliance	9	$pm^{-2}.N^{-1}$
s_{33}^{E}	Piezo short-circuit elastic compliance	20.7	$pm^{-2}.N^{-1}$
ε_{33}	Piezo dielectric constant	30	$nF.m^{-1}$
g_{33}	Piezo voltage constant	0.02	$V.m.N^{-1}$
K_{33}	Piezo Coupling Factor	0.75	-
W	Piezo width	0.4	mm
T	Piezo Thickness	0.8	mm
$A=W^2$	Piezo area	16×10^{-8}	m^2
$C_0 = A\varepsilon_{33}(1-K_{33}^{2})/T$	Piezo capacitance	2.6	pF
$v=\sqrt{\rho\, s_{33}^{D}}$	Piezo wave velocity	3851	$m.s^{-1}$
$\tau_c = T/v$	Piezo electrical length	208	ns
$N = g_{33}\varepsilon_{33}A/s_{33}^{E}\,T$	Piezo turn ratio	0.0057	---
$h=N/C_0$	Piezoelectric constant	2.192×10^{9}	$V.m^{-1}$
$Z_c = \rho v A$	Piezo radiation impedance	4.62	$Kg.s^{-1}$
ρ_t	Tissue density	1000	$Kg.m^{-3}$
v_t	Tissue wave velocity	1500	$m.s^{-1}$
d	Tissue layer thickness	20	mm
α	Tissue attenuation constant	95	$Np.m^{-1}$
$R=2\rho_t v_t A\alpha$	Tissue lossy line resistance	45.6	Ω
$L=A\rho_t$	Tissue lossy line inductance	160	μH
$C=1/Av_t^{2}$	Tissue lossy line capacitance	2800	μF

IV. RESULTS

The amplitude modulation of the backscattered signal was compared for two extreme values of electric load (R_L) in Fig. 4(a). The amplitude modulation of the echo is shown in Fig. 4(b). To establish the relationship between resistive load (R_L) and echo voltage (V_{echo}), RMS values of V_{echo} were plotted against R_L in Fig. 4(c). It can be seen that the echo voltage shows an increasing trend with the rising load resistance.

Backing layer acoustic impedance (Z_B) of the implant was also varied to find impedance at which the sensitivity of the backscattered amplitude fluctuations to the variations of the electrical load is maximum. This effect is shown in Fig. 4(d). It was noted that the echo voltage amplitude for constant R_L decreases with increasing impedance backing of the implant.

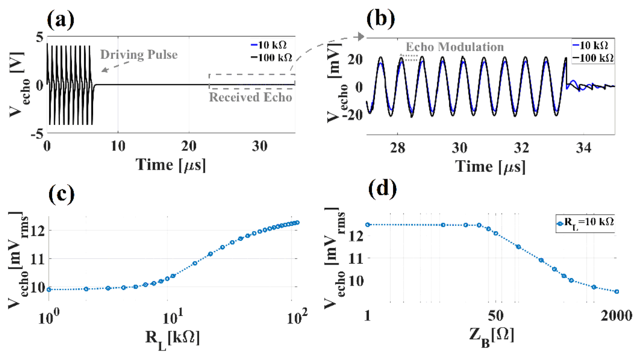

Fig. 4. (a) Driving pulse & transient response. (b) Echo amplitude variation with two extreme values of R_L. (c) RMS values of backscattered voltage vs. load impedance R_L. (d) RMS values of backscattered voltage vs. increasing Backing impedance Z_B.

The linear relationship between echo voltage amplitude and load impedance can be used to design and calibrate sensor response for modeling IMDs with sensors. This technique can also be applied to design ultrasonic-based, amplitude-modulated backscattering communication for various medical applications.

REFERENCES

[1] M. M. Ghanbari and R. Muller, “Optimizing Volumetric Efficiency and Backscatter Communication in Biosensing Ultrasonic Implants,” IEEE Trans. Biomed. Circuits Syst., pp. 1–12, 2020, doi: 10.1109/TBCAS.2020.3033488.

[2] D. Seo et al., “Wireless Recording in the Peripheral Nervous System with Ultrasonic Neural Dust NeuroResource Wireless Recording in the Peripheral Nervous System with Ultrasonic Neural Dust,” Neuron, vol. 91, no. 3, pp. 529–539, 2016, doi: 10.1016/j.neuron.2016.06.034.

[3] D. K. Piech et al., “neural stimulator with ultrasonically powered bidirectional communication,” Nat. Biomed. Eng., vol. 4, no. February, 2020, doi: 10.1038/s41551-020-0518-9.

[4] T. Energy et al., “Noninvasive Control of the Power Transferred to an Implanted Device by an Ultrasonic,” vol. 61, no. 4, pp. 995–1004, 2014.

[5] O. Shaul, S. Boaz, and S. Doron, “Non-invasive sensing of the electrical energy harvested by medical implants powered by an ultrasonic transcutaneous energy transfer link,” pp. 1153–1157, 2012.

[6] S. Ozeri and D. Shmilovitz, “Simultaneous backward data transmission and power harvesting in an ultrasonic transcutaneous energy transfer link employing acoustically dependent electric impedance modulation,” Ultrasonics, vol. 54, no. 7, pp. 1929–1937, 2014, doi: 10.1016/j.ultras.2014.04.019.

[7] D. B. Christensen and S. Roundy, “Power and Information Transmission to Implanted Medical Device Using Ultrasonic,” pp. 38–40, 2001.

[8] F. Mazzilli et al., “In-Vitro Platform to study Ultrasound as Source for Wireless Energy Transfer and Communication for Implanted Medical Devices,” pp. 3751–3754, 2010.

[9] W. P. Mason, Electromechanical Transducers and Wave Filters, 2nd ed. New Jersey: D. Van Nostrand Company, 1948.

[10] S. Sherrit, S. P. Leary, B. P. Dolgin, and Y. Bar-cohen, “Comparison of the Mason and KLM Equivalent Circuits for Piezoelectric Resonators in the Thickness Mode,” pp. 921–926, 1999.

[11] M. Redwood, “Transient Performance of a Piezoelectric Transducer,” J. Acoust. Soc. Am., vol. 33, no. 4, pp. 527–536, 1961.

[12] R. Krimholtz, D. A. Leedom, and G. L. Matthaei, “New Equivalent Circuits for Elementary Piezoelectric Transducers,” Electron Lett., vol. 6, no. 13, pp. 398–399, 1970.

[13] W. M. Leach, “Controlled-Source Analogous Circuits and SPICE Models for Piezoelectric Transducers,” IEEE Trans. Ultrason. Ferroelectr. Freq. Control, vol. 41, no. 1, pp. 60–66, 1994, doi: 10.1109/58.265821.

[14] D. Zheng, Y. Mao, Z. Cui, and S. Lv, “Optimization of Equivalent Circuit Model for Piezoelectric Ultrasonic Transducer,” 2018 IEEE Int. Instrum. Meas. Technol. Conf., pp. 1–5, 2018.